

## Binary nature of monolayer boron sheets from ab initio global searches

Haigang Lu, Yuewen Mu, Hui Bai, Qiang Chen, and Si-Dian Li

Citation: *J. Chem. Phys.* **138**, 024701 (2013); doi: 10.1063/1.4774082

View online: <http://dx.doi.org/10.1063/1.4774082>

View Table of Contents: <http://jcp.aip.org/resource/1/JCPSA6/v138/i2>

Published by the American Institute of Physics.

---

### Additional information on *J. Chem. Phys.*

Journal Homepage: <http://jcp.aip.org/>

Journal Information: [http://jcp.aip.org/about/about\\_the\\_journal](http://jcp.aip.org/about/about_the_journal)

Top downloads: [http://jcp.aip.org/features/most\\_downloaded](http://jcp.aip.org/features/most_downloaded)

Information for Authors: <http://jcp.aip.org/authors>

## ADVERTISEMENT



**Goodfellow**  
metals • ceramics • polymers • composites  
70,000 products  
450 different materials  
**small quantities fast**

[www.goodfellowusa.com](http://www.goodfellowusa.com)



## Binary nature of monolayer boron sheets from *ab initio* global searches

Haigang Lu,<sup>1,a)</sup> Yuewen Mu,<sup>2</sup> Hui Bai,<sup>1</sup> Qiang Chen,<sup>1</sup> and Si-Dian Li<sup>1,a)</sup>

<sup>1</sup>Key Laboratory of Chemical Biology and Molecular Engineering of the Education Ministry, Institute of Molecular Science, Shanxi University, Taiyuan, Shanxi 030006, People's Republic of China

<sup>2</sup>School of Physics and Electronic Engineering, Shanxi University, Taiyuan, Shanxi 030006, People's Republic of China

(Received 26 October 2012; accepted 13 December 2012; published online 9 January 2013)

Boron could be the next element after carbon to form two-dimensional monolayer structures. Using the *ab initio* global searches, we found all low-lying monolayer boron sheets with 1–4 hexagonal holes in each unit cell. The two most stable boron sheets are composed of two kinds of elementary units with isolated-hexagon and twin-hexagon holes, respectively, so that the boron sheets are binary structures in nature. Detailed structural analyses indicate that there exist two types of close-lying stable monolayer boron sheets, revealing the polymorphism of boron sheet. These binary monolayer boron sheets are expected to serve as precursors to build various boron nanotubes, boron fullerenes, and other boron-based low-dimensional nanomaterials. © 2013 American Institute of Physics. [<http://dx.doi.org/10.1063/1.4774082>]

### I. INTRODUCTION

Boron is an element with great chemical complexity due to its electron-deficiency property. Although there exist many forms of crystalline boron, such as  $\alpha$ -B<sub>12</sub>,  $\beta$ -B<sub>106</sub>, T-192, and  $\gamma$ -B<sub>28</sub>,<sup>1,2</sup> they all contain the same elementary unit of icosahedral B<sub>12</sub>. There has been no graphite-like layered boron reported to date. Furthermore, most of recently reported low-dimensional nanostructures, such as nanowires,<sup>3</sup> nanorods,<sup>4</sup> and nanoribbons,<sup>5,6</sup> also consist of icosahedral B<sub>12</sub> basic units.

As the light neighbor to carbon in the periodic table, boron could be the next element capable of forming two-dimensional (2D) monolayer structures. The successful syntheses of the single- and multi-walled boron nanotubes (MWBNTs)<sup>7,8</sup> suggest the possibility of producing monolayer boron sheets (BS) in experiments. Boron nanotubes can be viewed as rolling up a monolayered or multilayered boron sheet. High-resolution transmission electron microscopy experiments revealed that the spacing between two adjacent layers in MWBNTs is about 3.2 Å,<sup>8</sup> close to the interlayer spacing of 3.35 Å in graphite.<sup>9</sup> However, the  $\alpha$ -tetrahedral structure of MWBNTs proposed by Liu *et al.*<sup>8</sup> is still far from being conclusive for the reason that the synthesized MWBNTs were heavily mixed with boron nanowires.<sup>2,8</sup>

Various monolayer BS structures have been proposed using *ab initio* methods. By removing certain number of boron atoms from the monolayer triangular sheet, researchers have proposed several low-lying BS, such as  $\eta_{1/9}$ - ( $\alpha$ -),  $\eta_{2/15}$ -,  $\eta_{3/24}$ -,  $\eta_{1/8}$ -sheet ( $\alpha_1$ -), and  $\eta_{1/7}$ -sheet,<sup>10–14</sup> in which the “hexagonal hole density” ( $\eta_{m/n}$ ) is defined as the ratio of the number of hexagonal holes ( $m$ ) to the number of atoms ( $n$ ) of the original triangular sheet in the unit cell. The most stable BS proposed so far include the  $\eta_{1/9}$ -sheet by Tang *et al.*,<sup>10</sup>

$\eta_{3/24}$ - and  $\eta_{2/15}$ -sheets by Penev *et al.*,<sup>11</sup> and the  $\eta_{1/8}$ -sheet by Wu *et al.*<sup>12</sup> and by Yu *et al.*<sup>13</sup> These BS appear to lie so close in cohesive energies that they are expected to form polymorphs.<sup>11–13</sup> The chemical bonding analysis using the adaptive natural density partitioning (AdNDP) method<sup>15</sup> had shown that the hexagon holes are elementary structural units in these BS, which absorb the extra electrons from the filled hexagons.<sup>16</sup> It is also interesting to notice that, in addition to the uniformly distributed isolated-hexagon holes existing typically in  $\eta_{1/9}$ -,<sup>10</sup>  $\eta_{1/8}$ -,<sup>12,13</sup> and  $\eta_{1/7}$ -sheets,<sup>14</sup> the high stability of both  $\eta_{2/15}$ - and  $\eta_{3/24}$ -sheets<sup>11</sup> strongly suggests that twin-hexagon holes, i.e., two fused hexagonal holes, be stable elementary structural units in constructing 2D BS.

To obtain the most stable BS, several search methods were used, such as the cluster expansion method<sup>11</sup> and the particle-swarm optimization method.<sup>12,13</sup> However, these methods are not systematic and therefore cannot guarantee a thorough exploration of the configuration space. In the cluster method, the close-packed triangular sheet was decomposed into an inactive honeycomb sublattice and a triangular sublattice defined by the hexagon centers. The atoms in the inactive honeycomb sublattice could not be removed to form hexagonal holes.<sup>11</sup> In the particle-swarm optimization method, only unit cells with certain numbers of boron atoms (4, 6, 8, 10, 12, 14, and 16) were considered.<sup>12,13</sup> Due to the lack of experimental data at current stage, *ab initio* global searches remain the most reliable approach to predict the structural patterns of the most stable BS.

### II. COMPUTATIONAL METHODS

#### A. Density functional theory calculation

Our *ab initio* calculations were performed with the VASP5.2 package<sup>17,18</sup> using the projector augmented wave (PAW) method<sup>19</sup> in conjunction with the Perdew-Ernzerhof-Burke (PBE)<sup>20</sup> or the hybrid PBE0<sup>21</sup> functional and

<sup>a)</sup>Authors to whom correspondence should be addressed. Electronic addresses: luhg@sxu.edu.cn and lisidian@sxu.edu.cn.

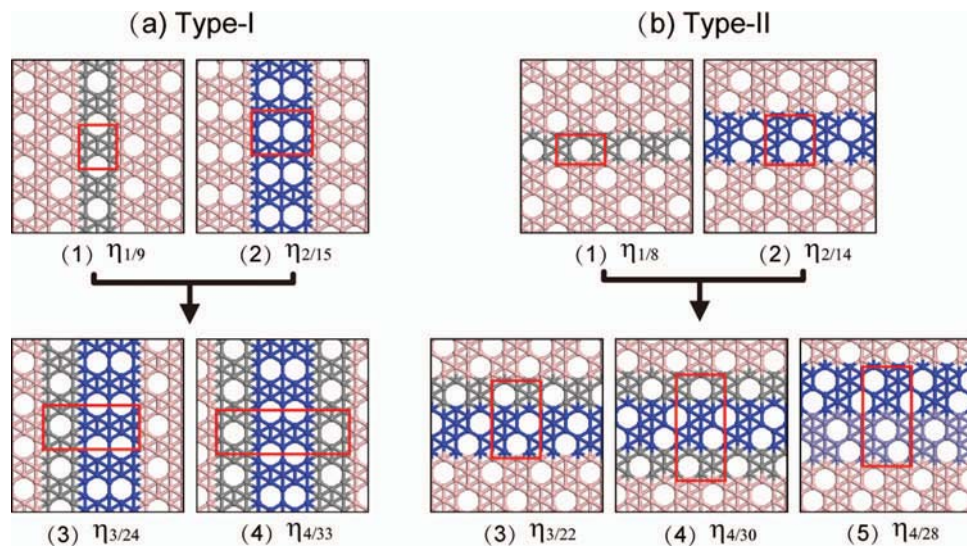


FIG. 1. Combinational relationships of type-I (a) and type-II (b) monolayer boron sheets. The grey fragments stand for  $\eta_{1/n}$ -units, the blue fragments for  $\eta_{2/n}$ -units, and the pearl blue fragment in (b)-(5) represent the reversed  $\eta_{2/14}$ -unit ( $\eta'_{2/14}$ -unit). The red solid rectangles show the schematic unit cells of the corresponding boron sheets.

employing a planewave basis set with a 500 eV kinetic energy cutoff. The Brillouin zone is sampled using k-points with  $0.02 \text{ \AA}^{-1}$  spacing in the Monkhorst-Pack scheme.<sup>22</sup> All BS are represented by unit cell with a  $30 \text{ \AA}$  vacuum region in the normal direction. For geometric optimization, both lattice constants and positions of atoms are fully relaxed. Upon optimization, the forces on all atoms are less than  $0.01 \text{ eV/\AA}$  and the criterion for total energy convergence is  $0.1 \text{ meV/atom}$ . The BS cohesive energy  $E_c = E_{\text{at}} - E_{\text{sheet}}$ , where  $E_{\text{at}}$  is the energy of an isolated spin-polarized boron atom and  $E_{\text{sheet}}$  is the energy per atom of a sheet using the PBE or hybrid PBE0 functionals.

## B. Global searching

The global search is based on a rectangle (about  $50 \text{ \AA} \times 50 \text{ \AA}$ ) of the monolayer triangular sheet (with the B-B bond length of  $r_{\text{B-B}} = 1.667 \text{ \AA}$ ). The BS with  $m$  holes ( $m = 1-4$ ) in each unit cell is successively yielded in the following five steps: (1) Select all possible supercells with  $n$  boron atoms ( $n = 2-40$ ) in the rectangle of triangular sheet, remove atoms at the vertexes, and convert the unit cell to its primitive cell by symmetrization using the FINDSYM module of ISOTROPY package.<sup>23</sup> By grouping the unit cells whose primitive cells have the same lattice constants and selecting a representative cell in each group, all unique  $\eta_{1/n}$ -BS ( $n = 2-40$ , about 350) with one hexagonal hole are obtained (see Fig. S1 in the supplementary material).<sup>24</sup> (2) In each  $\eta_{1/n}$ -BS, remove any atom nonadjacent with the hexagonal hole in turn to generate a series of  $\eta_{2/n}$ -BS. By grouping the  $\eta_{2/n}$ -BS unit cells which have the same PBE single-point energies using  $\Gamma$ -point and selecting a representative  $\eta_{2/n}$ -BS in each group, all unique  $\eta_{2/n}$ -BS (about 3600) are constructed. (3) According to Step (2), construct successively all the unique  $\eta_{3/n}$ -BS (about 26 000) and  $\eta_{4/n}$ -BS (about 220 000). (4) The single-point energies of these unique  $\eta_{m/n}$ -BS are evaluated using k-points with  $0.02 \text{ \AA}^{-1}$  spacing at the PBE level, and all the

$\eta_{m/n}$ -BS are sorted in cohesive energies per atom. (5) Finally, the 200 lowest-lying BS (including all the structures shown in Fig. 1 and Fig. S2 of the supplementary material<sup>24</sup>) are fully optimized and their cohesive energies are evaluated using the PBE functional. This procedure automatically produces all the previously reported most stable BS like  $\eta_{1/9}$ -,  $\eta_{1/7}$ -,  $\eta_{1/8}$ -,  $\eta_{2/15}$ -, and  $\eta_{3/24}$ -sheets.<sup>10-14</sup>

In the PBE optimized BS, the B-B bond lengths appear to be within the range of  $r_{\text{B-B}} = 1.67-1.70 \text{ \AA}$ , very close to the predefined B-B bond length of  $1.667 \text{ \AA}$  in the original triangular sheet. The stability order of the 200 BS after PBE optimization remains nearly same as that before optimization. Therefore, *ab initio* global searches performed in this work have located all the possible low-lying boron sheets based on the triangular boron sheet. Furthermore, the 20 lowest-lying BS are fully re-optimized and their cohesive energies are further refined using the more accurate PBE0 functional. The PBE0 cohesive energies are preferred to sort the lowest-lying BS based on the fact that the PBE0 functional was reported to be more reliable than the PBE functional for computing cohesive energy of bulk materials.<sup>25</sup>

## III. RESULTS AND DISCUSSION

All the lowest-lying  $\eta_{m/n}$  BS ( $m = 1-4$ ,  $n = 2-40$ ) lying within 10 meV contain isolated-hexagon and/or twin-hexagon hole(s) in their unit cells (see Fig. 1, Table I, and Fig. S2 of the supplementary material<sup>24</sup>). The most stable boron sheet obtained in this work at PBE0,  $\eta_{4/28}$ -sheet with the highest hexagonal hole density of  $\eta = 1/7$ , is composed of interconnected dumbbell-like planar  $D_{2h}$  B<sub>12</sub> units, with one pair of twin-hexagon holes in each unit cell. The second most stable boron sheet,  $\eta_{4/33}$ -sheet, consists of two kinds of fused planar hexagonal B<sub>7</sub> units ( $D_{2h}$  B<sub>7</sub> and  $C_{2v}$  B<sub>7</sub>), with two isolated-hexagon holes and one twin-hexagon hole in each unit cell. These structural characteristics suggest that the lowest-lying  $\eta_{4/28}$ - and  $\eta_{4/33}$ -sheets are combinations of certain elementary

TABLE I. Hexagonal hole density ( $\eta_{m/n}$ ), type of structures, cohesive energies  $E_c$  (eV) per atom at both PBE0 and PBE levels, and the combinational patterns of typical low-lying monolayer boron sheets with  $m$  ( $m = 1-4$ ) holes.

$\eta$	Type	$E_c$ (PBE0)	$E_c$ (PBE)	Combination
1/7		5.946	5.934	
1/8	II	5.976	5.954	
1/9	I	5.981	5.958	
1/10		5.930	5.915	
2/12		5.951	5.936	
2/13		5.962	5.939	
2/14	II	5.972	5.951	
2/15	I	5.982	5.958	
2/16		5.963	5.939	
3/20	II	5.969	5.945	
3/21	I	5.971	5.945	
3/22	II	5.982	5.955	$\eta_{1/8} \oplus \eta_{2/14}$
3/24	I	5.985	5.961	$\eta_{1/9} \oplus \eta_{2/15}$
4/28	II	5.987	5.957	$\eta_{2/14} \oplus \eta'_{2/14}$
4/30	II	5.979	5.955	$2\eta_{1/8} \oplus \eta_{2/14}$
4/33	I	5.986	5.961	$2\eta_{1/9} \oplus \eta_{2/15}$

units, similar to the icosahedral  $B_{12}$  elementary unit in crystalline boron.

To determine the elementary structural units of the planar BS, we investigated two series of low-lying BS:  $\eta_{1/n}$ -BS with an isolated-hexagon hole and  $\eta_{2/n}$ -BS with a twin-hexagon hole. As clearly shown in Fig. 2, the lowest-lying boron sheets with an isolated-hexagon hole in each unit cell are  $\eta_{1/9}$ - and  $\eta_{1/8}$ -sheets and those with a twin-hexagon hole are  $\eta_{2/15}$ - and  $\eta_{2/14}$ -sheets. Therefore, there are four best candidate elementary units for 2D boron sheets:  $\eta_{1/9}$ -,  $\eta_{1/8}$ -,  $\eta_{2/15}$ -, and  $\eta_{2/14}$ -units (a1, a2, b1, and b2 in Fig. 1).

The combinational relationships between the lowest-lying BS with 3 or 4 holes and their respective elementary units are shown in Fig. 1 with curved arrows. Close

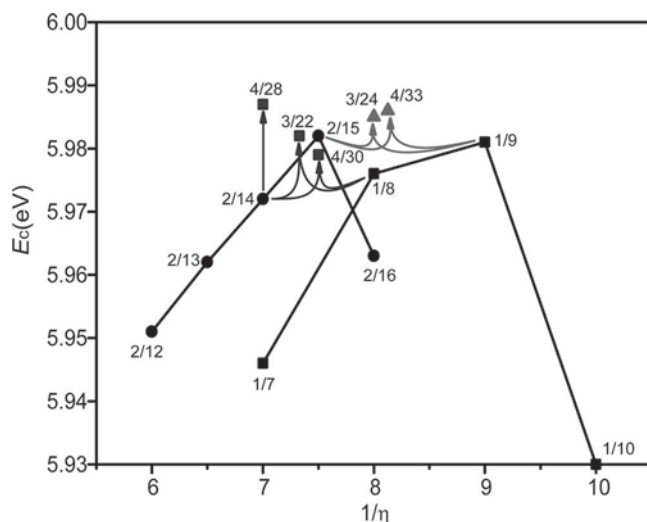


FIG. 2. Cohesive energies ( $E_c$ ) vs reciprocal hexagonal hole density ( $1/\eta$ ) for the lowest-lying boron sheets with an isolated-hexagon or twin-hexagon hole. The curved arrows show the combinational relationships of the type-I and type-II sheets with 3 or 4 hexagonal holes with their component elementary units.

structural analyses indicate that the  $\eta_{1/9}$ - and  $\eta_{2/15}$ -units combine to form the  $\eta_{3/24}$ -sheet ( $\eta_{1/9} \oplus \eta_{2/15}$ ) and  $\eta_{4/33}$ -sheet ( $2\eta_{1/9} \oplus \eta_{2/15}$ ) (Fig. 1(a)), while the  $\eta_{1/8}$ - and  $\eta_{2/14}$ -units combine to form the  $\eta_{3/22}$ -sheet ( $\eta_{1/8} \oplus \eta_{2/14}$ ) and  $\eta_{4/30}$ -sheet ( $2\eta_{1/8} \oplus \eta_{2/14}$ ) (Fig. 1(b)). Interestingly, the most stable  $\eta_{4/28}$ -sheet appears to be a 1:1 combination between the  $\eta_{2/14}$ -unit and its reversed  $\eta'_{2/14}$ -unit ( $\eta_{2/14} \oplus \eta'_{2/14}$ ) (Fig. 1(b)(5)). Thus, the  $\eta_{1/9}$ -,  $\eta_{2/15}$ -,  $\eta_{1/8}$ -, and  $\eta_{2/14}$ -units are *indeed* the elementary units of the lowest-lying BS with 1–4 hexagonal holes obtained through global searches.

There exists two types of structural patterns in these lowest-lying BS: type-I including  $\eta_{3/24}$ - and  $\eta_{4/33}$ -BS (see Fig. 1(a)) which are combinations of the  $\eta_{1/9}$ - and  $\eta_{2/15}$ -units in direction parallel to the extended –B–B– chains and type-II including  $\eta_{3/22}$ -,  $\eta_{4/28}$ -, and  $\eta_{4/30}$ -BS (see Fig. 1(b)) which are hybrids of the  $\eta_{1/8}$ - and  $\eta_{2/14}$ -units in direction perpendicular to the extended –B–B– chains. Elementary units within the same type can be combined to form seamless boron sheets with more hexagonal holes in each unit cell. Two infinite series of binary boron sheets can be constructed in these patterns, with type-I in the formula of  $n\eta_{1/9} \oplus m\eta_{2/15}$ -BS ( $n = 1, 2, \dots$  and  $m = 1, 2, \dots$ ) and type-II in the formula of  $n\eta_{1/8} \oplus m\eta_{2/14} \oplus l\eta'_{2/14}$ -BS ( $n = 0, 1, 2, \dots$ ,  $m = 1, 2, \dots$ , and  $l = 0, 1, 2, \dots$ ).

As shown in Figs. 1 and 2 and Table I, the combination of different elementary units produces binary boron sheets with higher cohesive energies than either of their component elementary units. For example, the most stable  $\eta_{4/28}$ -sheet is 15 meV per atom more stable than its component  $\eta_{2/14}$ -unit (and  $\eta'_{2/14}$ -unit) in cohesive energy, while the second most stable  $\eta_{4/33}$ -sheet lies 4 meV and 5 meV lower than the  $\eta_{2/15}$ - and  $\eta_{1/9}$ -units, respectively.

According to the combinational formulae presented above, we constructed new BS with more than four hexagonal holes in each unit cell: type-I BS with 5–7 hexagonal holes ( $\eta_{5/39}$ ,  $\eta_{5/42}$ ,  $\eta_{6/48}$ ,  $\eta_{6/51}$ ,  $\eta_{7/54}$ ,  $\eta_{7/57}$ , and  $\eta_{7/60}$ , see Fig. S3 in the supplementary material<sup>24</sup>) and type-II BS with 5 and 6 hexagonal holes ( $\eta_{5/36}$ ,  $\eta'_{5/36}$ ,  $\eta_{5/38}$ ,  $\eta'_{6/42}$ ,  $\eta_{6/44}$ ,  $\eta'_{6/44}$ , and  $\eta_{6/46}$ , see Fig. S4 in the supplementary material<sup>24</sup>). The type-I cohesive energies (5.960–5.961 eV) appear to be nearly equal to that of  $\eta_{4/33}$ -BS (5.961 eV) and type-II ones (5.953–5.956 eV) approximate to that of  $\eta_{4/28}$ -BS (5.957 eV) at the PBE level. Type-I and type-II BS with more than four hexagonal holes lie very close in thermodynamic stabilities with  $\eta_{4/33}$ -BS and  $\eta_{4/28}$ -BS, respectively, and as the sizes of unit cell increase, the cohesive energies of boron sheets converge gradually (see Table I and Figs. S2–S4 in the supplementary material<sup>24</sup>). As such combinations can be extended to infinity, two types of polymorphous boron sheets may be formed in the type-I and type-II configurational space, respectively, with each consisting of two elementary units. Such structural patterns clearly reveal the binary nature of polymorphous boron sheets.

There are two other possible elementary units with a triplet-hexagon hole: type-I  $\eta_{3/21}$ - and type-II  $\eta_{3/20}$ -units (see Figs. S5 and S6 in the supplementary material<sup>24</sup>). It is difficult for  $\eta_{3/21}$ -unit to participate in type-I BS because the cohesive energies of  $\eta_{3/21}$ -BS and its combinations ( $\eta_{4/30}$ - and  $\eta_{5/36}$ -BS) lie about 9 meV per atom higher than that of  $\eta_{4/33}$ -BS (Fig. S5 in the supplementary material<sup>24</sup>). The  $\eta_{3/20}$ -BS is

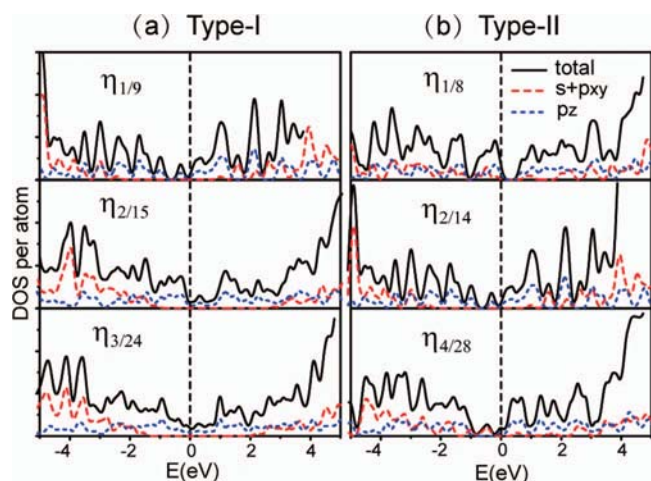


FIG. 3. DOS and PDOS for some representative type-I (a) and type-II (b) boron sheets. Projections are onto in-plane (sum of  $s$ ,  $p_x$ , and  $p_y$ , dashed red) and out-of-plane orbitals ( $p_z$ , dotted blue). The vertical dashed lines show the Fermi energy ( $E_F$ ). (We use 0.1 eV of GAUSSIAN broadening. The vertical scale is arbitrary.)

expected to make minor contribution to type-II BS for the reason that its lowest-energy combination,  $\eta'_{5/34}$ -BS, is 4 meV less stable than the most stable  $\eta_{4/28}$ -BS (Fig. S6 in the supplementary material<sup>24</sup>).

The stability of the type-I and type-II BS originates from their elementary units,  $\eta_{1/9}$ -,  $\eta_{2/15}$ -,  $\eta_{1/8}$ -, and  $\eta_{2/14}$ -units, of which the former three were investigated previously,<sup>10–13</sup> while the last one  $\eta_{2/14}$ -unit is obtained for the first time in this work. Figure 3 shows densities of states (DOS) and projected densities of states (PDOS) at PBE0 level for six representative BS (type-I  $\eta_{1/9}$ -,  $\eta_{2/15}$ -, and  $\eta_{3/24}$ -BS, and type-II  $\eta_{1/8}$ -,  $\eta_{2/14}$ -, and  $\eta_{4/28}$ -BS) with separate in-plane ( $\sigma_{s+pxy}$ ) and out-of-plane ( $\pi_{pz}$ ) projections. It is true that, as indicated by Tang and Ismail-Beigi and confirmed by Penev *et al.* and Wu *et al.*,<sup>10–12</sup> all the stable binary BS have the Fermi levels located within the gaps of the in-plane derived PDOS ( $\sigma_{s+pxy}$ ) so that all  $\sigma$  bonding states are filled, while their  $\sigma$  antibonding ones remain empty. However, as indicated in Fig. 3, the out-of-plane induced PDOS ( $\pi_{pz}$ ) and therefore the total DOS of these stable boron sheets possess non-zero values at their Fermi levels, showing that there are certain occupations in their delocalized out-of-plane induced  $\pi$ -states. Thus, these binary boron sheets are predicted to be metallic in their  $p_z$ -derived bands.

The measured interlayer distance from MWBNTs<sup>8</sup> is an indirect evidence of the weak van der Waals interaction between neighboring boron layers. We employed the PBE method including dispersion correction (DFT-D2)<sup>26</sup> to account for the weak interlayer interaction between two monolayer boron sheets. The average optimized interlayer distances in the AB stacking bilayer  $\eta_{4/28}$ - and  $\eta_{4/33}$ -BS (see Fig. S7 in the supplementary material<sup>24</sup>) appeared to be 3.16 and 3.04 Å,

respectively, both in good agreement with the measured interlayer distance of 3.2 Å in MWBNTs.<sup>8</sup>

#### IV. CONCLUSIONS

Using the *ab initio* global searches, all low-lying BS with 1–4 hexagonal holes in each unit cell have been located in this work. Detailed structural analyses indicate that there exist two types of close-lying stable monolayer boron sheets, type-I with  $\eta_{1/9}$ - and  $\eta_{2/15}$ -units and type-II with  $\eta_{1/8}$ - and  $\eta_{2/14}$ -units, respectively, unraveling the binary nature of 2D boron sheets. The two structural patterns have been employed to construct monolayer boron sheets with up to 7 hexagonal holes in each unit cell. Both the AB stacking bilayer  $\eta_{4/28}$ - and  $\eta_{4/33}$ -sheets are found to possess the calculated interlayer distances in good agreement with the measured value in MWBNTs. These binary monolayer boron sheets predicted at *ab initio* levels are expected to serve as precursors to build various boron nanotubes, boron fullerenes, and other boron-based low-dimensional nanomaterials.

<sup>1</sup>A. R. Oganov, J. Chen, C. Gatti, Y. Ma, Y. Ma, C. W. Glass, Z. Liu, T. Yu, O. O. Kurakevych, and V. L. Solozhenko, *Nature* **457**, 863 (2009).

<sup>2</sup>I. Boustani, *Chem. Modell.* **8**, 1 (2011).

<sup>3</sup>J. Tian, C. Hui, L. Bao, C. Li, Y. Tian, H. Ding, C. Shen, and H. Gao, *Appl. Phys. Lett.* **94**, 083101 (2009).

<sup>4</sup>D. M. Zhu and E. Kisi, *J. Aust. Ceram. Soc.* **45**, 49 (2009), available online at <http://www.austceram.com/JAC-2009/ACS-Journal-2009-Zhu.htm>.

<sup>5</sup>T. T. Xu, J. Zheng, N. Wu, A. W. Nicholls, J. R. Roth, D. A. Dikin, and R. S. Ruoff, *Nano Lett.* **4**, 963 (2004).

<sup>6</sup>Y. Ding, X. Yang, and J. Ni, *Appl. Phys. Lett.* **93**, 043107 (2008).

<sup>7</sup>D. Ciuparu, R. F. Klie, Y. M. Zhu, and L. Pfefferle, *J. Phys. Chem. B* **108**, 3967 (2004).

<sup>8</sup>F. Liu, C. Shen, Z. Su, X. Ding, S. Deng, J. Chen, N. Xu, and H. Gao, *J. Mater. Chem.* **20**, 2197 (2010).

<sup>9</sup>P. Delhaes, *Graphite and Precursors* (CRC, 2001).

<sup>10</sup>H. Tang and S. Ismail-Beigi, *Phys. Rev. Lett.* **99**, 115501 (2007).

<sup>11</sup>E. S. Penev, S. Bhowmick, A. Sadrzadeh, and A. I. Yakobson, *Nano Lett.* **12**, 2441 (2012).

<sup>12</sup>X. J. Wu, J. Dai, Y. Zhao, Z. W. Zhuo, J. L. Yang, and X. C. Zeng, *ACS Nano* **6**, 7443 (2012).

<sup>13</sup>X. Yu, L. Li, X. Xu, and C. Tang, *J. Phys. Chem. C* **116**, 20075 (2012).

<sup>14</sup>R. R. Zope and T. Baruah, *Chem. Phys. Lett.* **501**, 193 (2011).

<sup>15</sup>D. Yu. Zubarev and A. I. Boldyrev, *Phys. Chem. Chem. Phys.* **10**, 5207 (2008).

<sup>16</sup>T. R. Galeev, Q. Chen, J.-C. Guo, H. Bai, C.-Q. Miao, H.-G. Lu, A. P. Sergeeva, S.-D. Li, and A. I. Boldyrev, *Phys. Chem. Chem. Phys.* **13**, 11575 (2011).

<sup>17</sup>G. Kresse and J. Furthmüller, *J. Comput. Mater. Sci.* **6**, 15 (1996).

<sup>18</sup>G. Kresse and J. Furthmüller, *Phys. Rev. B* **54**, 11169 (1996).

<sup>19</sup>P. E. Blöchl, *Phys. Rev. B* **50**, 17953 (1994).

<sup>20</sup>J. P. Perdew, K. Burke, and M. Ernzerhof, *Phys. Rev. Lett.* **77**, 3865 (1996).

<sup>21</sup>J. P. Perdew, M. Ernzerhof, and K. Burke, *J. Chem. Phys.* **105**, 9982 (1996).

<sup>22</sup>H. J. Monkhorst and J. D. Pack, *Phys. Rev. B* **13**, 5188 (1976).

<sup>23</sup>H. T. Stokes, D. M. Hatch, and B. J. Campbell, isotropy (2007), see <http://stokes.byu.edu/isotropy.html>.

<sup>24</sup>See supplementary material at <http://dx.doi.org/10.1063/1.4774082> for construction of boron sheets, some low-lying  $\eta_{m/n}$  boron sheets with  $m = 1-7$  and  $n = 7-60$ , and AB stacking bilayer boron sheets of  $\eta_{4/28}$ - and  $\eta_{4/33}$ -sheets.

<sup>25</sup>C. Adamo and V. Barone, *J. Chem. Phys.* **110**, 6158 (1999).

<sup>26</sup>S. Grimme, *J. Comp. Chem.* **27**, 1787 (2006).